Effect of yttrium addition on the formation and mechanical properties of Ti–Zr–Ni–Cu bulk quasicrystalline alloys

Xinlu Wang [a,b], Shanshan Zhang [a,c], Lidong Wang [a], Wanqiang Liu [a,c], Yaoming Wu [a], Limin Wang [a,*]

[a] State Key Laboratory of Rare Earth Resource Utilization, Changchun Institute of Applied Chemistry, CAS, Changchun 130022, China
[b] Graduate University of the Chinese Academy of Sciences, Beijing 100049, China
[c] School of Materials science and Engineering, Changchun University of Science and Technology, Changchun 130022, China

A B S T R A C T

The effect of yttrium (Y) on the structure and mechanical properties of the as-cast $(Ti_{48}Zr_{36}Ni_{14}Cu_2)_{1-x}Y_x$ ($x = 0$, 0.01 and 0.02) bulk quasicrystalline alloys was investigated. These alloys were mainly composed of icosahedral quasicrystalline phase (i-phase) accompanied by minor hexagonal C14 Laves phase and solid-solution β-(Ti/Zr) phase. The characterization on their mechanical properties had been carried out by means of microhardness indentation and compression tests at room temperature. The microhardness test showed that the toughness of them was much better than many other i-phase alloys because no obvious crack was detected even at the load of 4.9 N. The compressive fracture strengths first increased and then decreased with increasing x, and the highest strength was 1350 MPa when $x = 0.01$, it was 210 MPa higher than the without Y alloy. These results reveal that an appropriate amount of Y addition would enhance the mechanical properties of the bulk i-phase alloy.

© 2012 Elsevier B.V. All rights reserved.

1. Introduction

In 1984, a revolutionary discovery of icosahedral quasicrystalline phase in Al–Mn alloy by Shechtman et al. [1], with both long-range aperiodic order and crystallographically forbidden rotational symmetries, opens a new branch of solid state physics and arouses extensive studies on a wide range of quasicrystalline alloys. It is reported that the initial studies of Ti-based i-phase alloys mainly concentrate in metastable quasicrystals [2], until Kelton et al. found a thermodynamically stable and well-ordered i-phase in the Ti–Zr–Ni alloy [3], which makes it possible to study the physical/mechanical properties of the bulk i-phase. To address this issue, the previous researches found that the Ti–Zr–Ni–Cu i-phase alloys have a good forming ability, higher mechanical properties and special hydrogen storage ability. The compressive strength of bulk $Ti_{45}Zr_{35}Ni_{17}Cu_3$ i-phase alloy could achieve to 1030 MPa [4], informing that the Ti–Zr–Ni–Cu quasicrystal deserves further comprehensive study on the enhancement of its mechanical properties.

Known as "industry vitamin", rare earth element can be used in a wide variety of materials to improve their qualities and performances, due to its excellent optical, electrical, magnetic and mechanical properties. However, the effect of rare earth elements on the formation ability of Ti-based i-phase alloy has scarcely received attention, until recently Wang et al. [5–7] reported the effect of Y and La on the phase structure and electrochemical hydrogen storage properties of the melt-spun Ti–Zr–Ni i-phase alloys. The results showed that both the intensity of the diffraction peak corresponding to i-phase and the maximum discharge capacity decreased with increasing the content of rare earth elements. While Matsumoto et al. [8,9] demonstrated that Y improved the i-phase forming ability of $Ti_{45}Zr_{38}Ni_{17}$ alloy by reducing the oxygen content in the matrix of the milled powder during the mechanical alloying. In the present work, we systematically investigate the effect on the structures and mechanical properties of the as-cast $Ti_{48}Zr_{36}Ni_{14}Cu_2$ i-phase alloy by adding Y element.

2. Experimental procedures

Alloy ingots with nominal composition of $(Ti_{48}Zr_{36}Ni_{14}Cu_2)_{1-x}Y_x$ ($x = 0$, 0.01 and 0.02), were prepared by arc-melting mixtures of 99.9% pure elements on a water-cooled Cu hearth in a high-purity Ar gas atmosphere. The master alloys were re-melted four times for chemical homogeneity. Cylindrical rods with 3 mm diameter and 70 mm length were prepared by squeezing the melt into a copper mould using a modified melt-spinner. The ingots were heated to melting in Ar-atmosphere and squeezed out of the quartz nozzle with 0.04 MPa argon overpressure.

The microstructures were characterized by X-ray diffraction (XRD) with Cu-Kα radiation and electron microscopy. Transmission electron microscopy (TEM) and

* Corresponding author. Tel.: +86 431 85262447; fax: +86 431 85262447.
E-mail addresses: wxl@ciac.jl.cn, xinluwang@163.com (X. Wang),
lmwang@ciac.jl.cn (L. Wang).
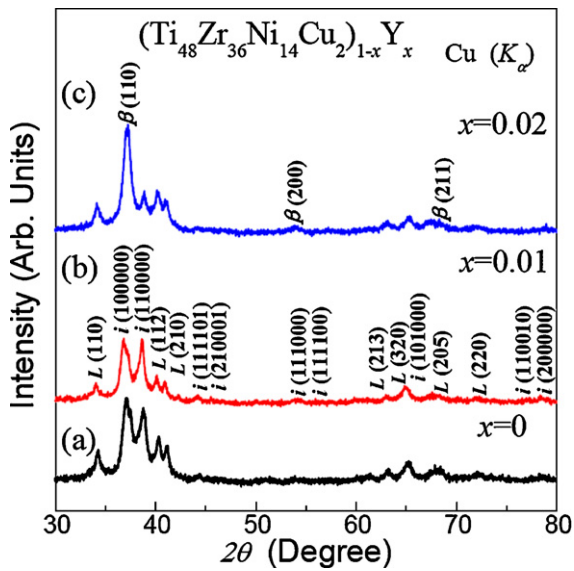
Fig. 1. X-ray diffraction patterns of the as-cast $(Ti_{48}Zr_{36}Ni_{14}Cu_2)_{1-x}Y_x$ ($x = 0$, 0.01 and 0.02) alloys: i, i-phase; L, C14 Laves phase; β, β-(Ti/Zr) solid solution phase.

High-resolution transmission electron microscopy (HRTEM) investigations were performed using a JEM-2100F microscope with 200 kV acceleration voltages. TEM specimens were thinned by argon ion milling techniques. A FEI-XL30 scanning electron microscope (SEM) was used for fracture surface analysis. Room temperature uniaxial compression tests on cylindrical specimens (3.0 mm diameter and 6.0 mm long) were done with an Instron-type testing device under quasistatic loading at an initial strain rate of 0.5 mm/min, and the Vickers microhardness (Hv) was examined using a FM-700 microhardness tester for a loading time of 15 s under the load of 0.98, 2.94, 4.9 and 9.8 N. Values of the hardness were averaged from 10 measurements.

3. Results and discussion

3.1. Phase structure

Fig. 1 shows XRD patterns of the $(Ti_{48}Zr_{36}Ni_{14}Cu_2)_{1-x}Y_x$ as-cast cylindrical rods with the diameter of 3 mm. The peaks of i-phase can be indexed according to the scheme first proposed by Bancel et al. [10]. Seen from Fig. 1(a), it could be observed i-phase together with a little quantity of hexagonal C14 Laves phase (L-phase). The i-phase peaks become sharper and more intense when $x = 0.01$ as shown in Fig. 1(b), although accompanied by minor L-phase peaks. However, further increasing the amount of Y leads to the appearance of bcc solid-solution β-(Ti/Zr) phase, coexisted with i-phase and L-phase
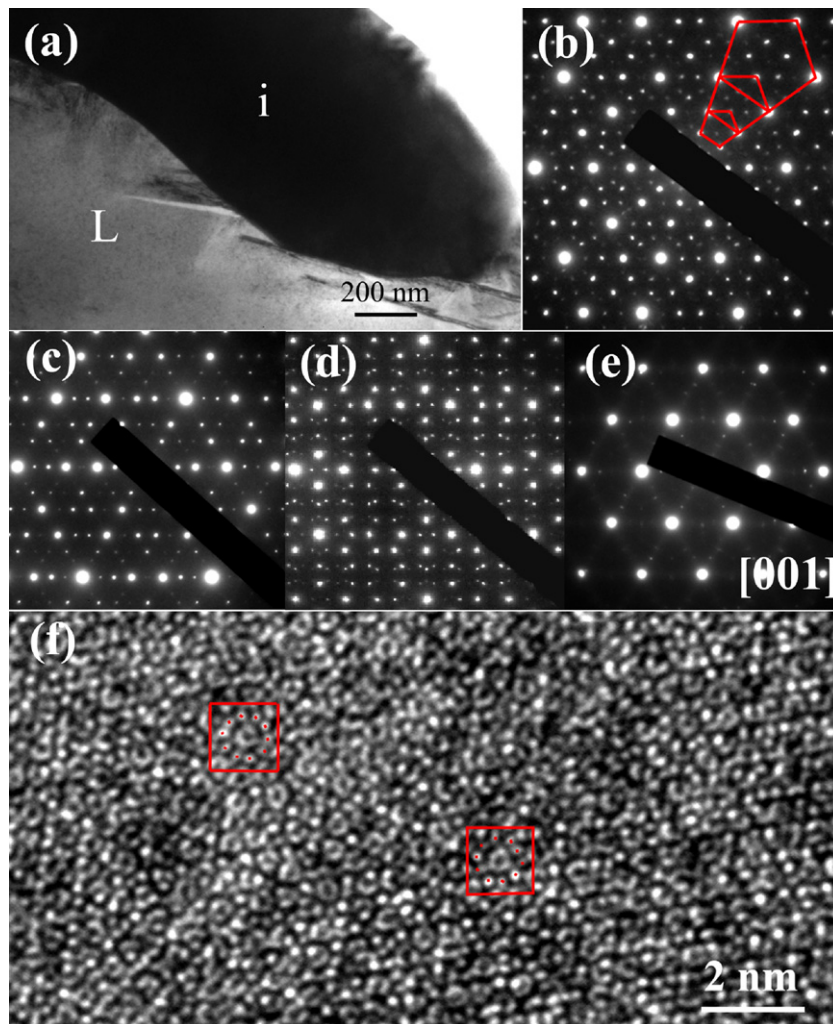
Fig. 2. (a) TEM image of the as-cast $(Ti_{48}Zr_{36}Ni_{14}Cu_2)_{0.99}Y_{0.01}$ with its (b) fivefold, (c) threefold and (d) twofold symmetries of the i-phase and its (e) [0 0 1] electron diffraction pattern of the C14 Laves phase. (f) High-resolution analysis of the i-phase.
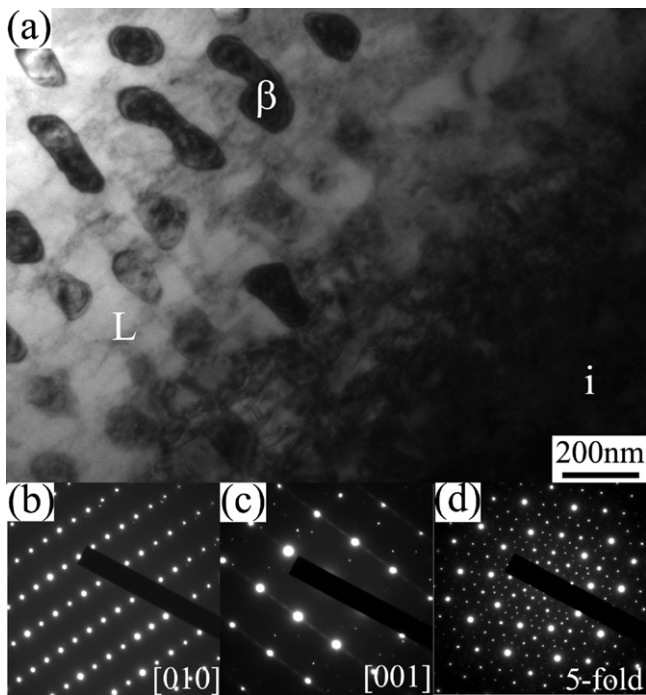
Fig. 3. (a) TEM image of the as-cast $(Ti_{48}Zr_{36}Ni_{14}Cu_2)_{0.98}Y_{0.02}$ with its (b) [0 1 0] electron diffraction pattern of the C14 Laves phase, (c) [0 0 1] electron diffraction pattern of the β-(Ti/Zr) phase and its (d) fivefold symmetries of the i-phase.

(Fig. 1c). These results suggest that the appropriate Y addition, to some degree, can improve the quasicrystal-forming ability in the quinary alloy system. During the preparation of the alloy, metal oxide on the surface of starting element metals and residual oxygen in the melting atmosphere are inevitably incorporated. However, oxygen is a definitely deterrent to i-phase formation in Ti–Zr–Ni alloys [11]. Owing to its strong oxygen affinity, the Y could remove the oxygen in the $Ti_{48}Zr_{36}Ni_{14}Cu_2$ alloy to facilitate the formation of quasicrystals. On the other hand, according to Darken–Garry theory, the intermetallic compounds can be formed easily when the atomic radius ratio is less than 85% and the electronegativity difference is more than 0.4 [12], thus excessive Y addition might form some stable compounds with Ni or Cu. This might result in the solid-solution β-(Ti/Zr) phase increased due to decreasing the Ni/Cu content in the local molten alloys.

The conventional XRD alone is not enough to distinguish phases in these alloys, because previous calculations have shown that the powder patterns from high-order crystal approximants which form with local icosahedral symmetry closely resemble those from the true i-phase [13,14]. Fortunately, differences between the two phases are often evident in electron diffraction patterns obtained by TEM [15]. Thus we performed a TEM examination of the $(Ti_{48}Zr_{36}Ni_{14}Cu_2)_{1-x}Y_x$ as-cast alloys. In agreement with the XRD results, when $x = 0.01$, the gray L-phase corresponding to a characteristic [0 0 1] orientation (Fig. 2e) and the dark i-phase are displayed in the bright-field image, as shown in Fig. 2(a). Different from the mottled and faceted appearance in rapid-quenching experiments [13], the grains of i-phase are larger in
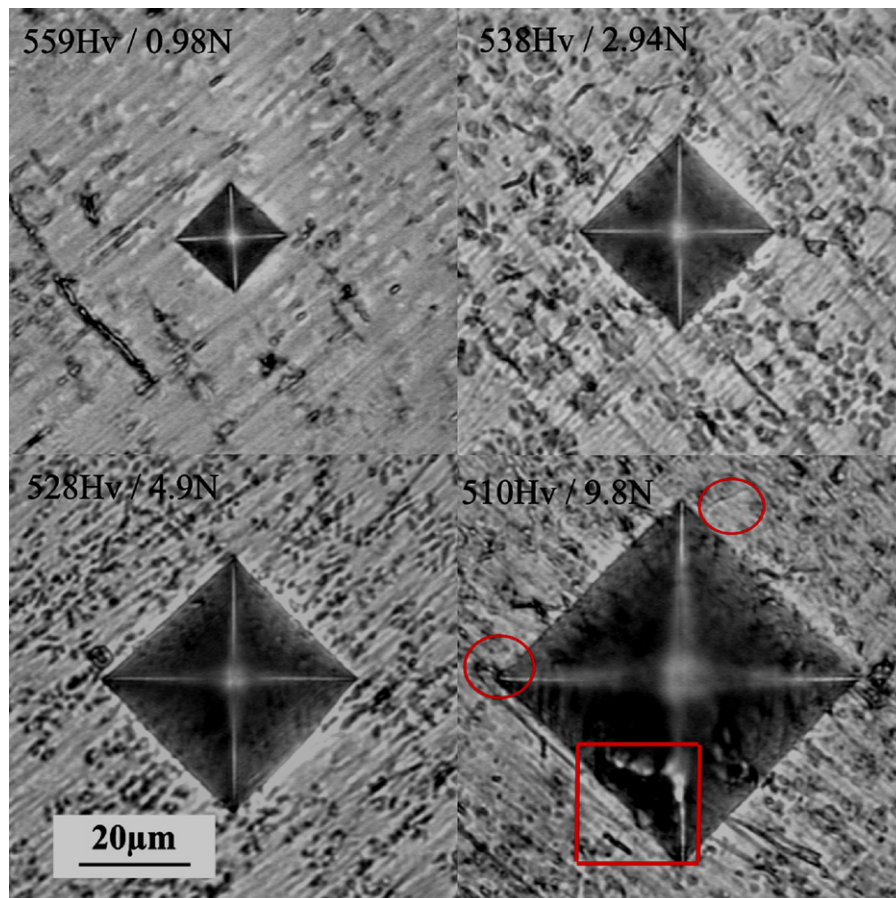
Fig. 4. The typical indentations of the bulk $(Ti_{48}Zr_{36}Ni_{14}Cu_2)_{0.99}Y_{0.01}$ alloy under different loads.

this as-cast alloy, since the slower cooling rate providing time for grain grown. In diffraction studies for the point-group symmetry of the i-phase, the expected representative electron diffraction patterns along fivefold $[-1,\tau,0]$, threefold $[-\tau^2,1,0]$ and twofold $[0,1,0]$ are observed in Fig. 2(b)–(d) respectively, which is indexed following Chattopadhyay et al. [16]. No evidence of the strong localized diffuse scattering, generally existed in rapidly quenched Ti–TM–Si–O (TM = transition metal) [17] and Ti–Zr–Fe [18] i-phase alloys, is observed in the selected-area diffraction patterns shown in Fig. 2(b)–(d), indicating that these quasicrystals are reasonably ordered. A HRTEM image parallel to the fivefold axis is shown in Fig. 2(f). It is obvious that there are many decagonally arranged spots and some of these sets are marked with small dots in a red frame. Additionally, no translational symmetry could be found in the whole area observed, although these bright dots more or less lie on parallel lines. Consistent with the XRD measurements in Fig. 1(c), the TEM image of the alloy with $x = 0.02$ shown in Fig. 3 reveals that the inserted diffraction patterns have a [0 1 0] orientation of the L-phase, a [0 0 1] orientation of the β-(Ti/Zr) phase and the fivefold symmetry of the i-phase. As shown in Fig. 3(a), it is found that the cell-like dark β-(Ti/Zr) phase is frequently surrounded by gray L-phase. The grain size of cell-like phase is approximately 60–300 nm.

3.2. Mechanical properties

Hardness measurement is a composite indicator to characterize the mechanical properties especially for the brittle materials. The indentations experiments of $(Ti_{48}Zr_{36}Ni_{14}Cu_2)_{1-x}Y_x$ alloys are carried out at four different loads namely 0.98, 2.94, 4.9 and 9.8 N. It is found that the hardness of all these samples decreases with the load increasing. The representative load-hardness behavior of $(Ti_{48}Zr_{36}Ni_{14}Cu_2)_{0.99}Y_{0.01}$ alloy is presented in Fig. 4. The typical dependence between hardness and applied load, which is known as the indentation size effect, has been extensively reviewed on conventional crystalline materials [19], and reported on Al–Cu–Co quasicrystals [20] and $Ti_{41.5}Zr_{41.5}Ni_{17}$ quasicrystals [22]. When performed on brittle materials (e.g. i-phase alloys), hardness indentation can generate cracks. For instance, the crack could occur at the edge of the indention of Al-based i-phase alloy when the load of Hv testing was larger than 0.49 N [21]. Yi et al. [22] have investigated the Hv of the $Ti_{41.5}Zr_{41.5}Ni_{17}$ bulk I-phase alloy prepared by hot-pressing method, the cracks were observed when the load was more than 1.0 N, and obvious radial and lateral cracks appeared at a load of 2 and 10 N. Liu et al. [4] found several radial cracks near the corner of the indenter mark when the load is increasing to 4.90 N for $Ti_{45}Zr_{35}Ni_{17}Cu_3$ icosahedral quasicrystalline alloy. However, different from above results, no crack is observed in $(Ti_{48}Zr_{36}Ni_{14}Cu_2)_{1-x}Y_x$ alloys when the load increases to 4.9 N, whereas several radial and lateral cracks are found near the corner of the indenter mark further increase to 9.8 N, as the typical

indentations of the alloy $x = 0.01$ manifested in Fig. 4. It reveals that the toughness of the Ti–Zr–Ni–Cu–Y bulk alloys are slightly better than the other Ti-based i-phase alloys like $Ti_{41.5}Zr_{41.5}Ni_{17}$ [22] and $Ti_{45}Zr_{35}Ni_{17}Cu_3$ [4], while much better than Al-based i-phase alloy [21].

Table 1 summarizes the Hv, compressive fracture strength (σ_f), deformation (ε) and Young's modulus (E) of the bulk $(Ti_{48}Zr_{36}Ni_{14}Cu_2)_{1-x}Y_x$ alloys and other Ti-based i-phase alloys. Similar characteristics are found in these alloys, namely, they have high Hv and low E. The values of Hv tests performed on Ti–Zr–Ni–Cu–Y alloys under the load of 4.9 N are 509, 528 and 537 respectively with the Y content increasing. The compressive fracture strength first increases and then slightly decreases with increasing x from 0 to 0.02. The highest strength is 1351 MPa when $x = 0.01$, which is 210 MPa higher than the alloy without Y and higher than the other Ti-based bulk i-phase alloys [22–24]. It is clear that the hardness and fracture strength of Y addition alloys are higher than without Y alloy. The possible reasons are as follows. Firstly, appropriate Y addition could reduce impurities in the matrix or impurities segregation to grain boundaries by forming some harmless compounds contained impurities. This could inhibit the structure loose which induced by impurities, and further improve the hardness and strength of the alloys. Secondly, a portion of Y elements would diffuse into the alloy matrix which is mainly composed of i-phase and L-phase, and produce the solid-solution strengthening effect. In addition, as seen from the TEM image (Fig. 3), small size β-(Ti/Zr) phase are scattered in alloy matrix when Y addition is 0.02, which may lead to dispersion strengthening. Moreover, since various phases have different structures and elasticity modulus, too many phases in the $(Ti_{48}Zr_{36}Ni_{14}Cu_2)_{0.98}Y_{0.02}$ alloy will increase the inhomogeneity of elastic deformation, and result in premature fracture. Therefore, the fracture strength of three-phase alloy with $x = 0.02$ is lower than two-phase alloy with $x = 0.01$.

Furthermore, the present bulk i-phase alloy exhibits a much lower Young's modulus (21.7 GPa) comparing with the Al-based ones [25,26]. This phenomenon is in agreement with the results reported by Ponkratz et al. [27], who found that the Ti–Zr–Ni i-phase alloy had high Poisson's ratio of 0.48 ± 0.015, and Young's modulus range of the Ti–Zr–Ni i-phase alloy was 5–35 GPa. The compressive curves of the bulk $(Ti_{48}Zr_{36}Ni_{14}Cu_2)_{1-x}Y_x$ alloys indicate that all samples undergo the elastic deformation without plastic deformation (Fig. 5). Likewise, the compressive specimens break into multiple pieces with irregular shapes and their fracture surfaces present similar appearance. The fractography of the bulk $(Ti_{48}Zr_{36}Ni_{14}Cu_2)_{0.99}Y_{0.01}$ alloy is shown in Fig. 6. It presents obvious river-like pattern and many cleavage planes which suggest that the fracture mold of this alloy is brittle cleavage fracture. The arrows show the main cracks existed in the fracture surface. It is found that the direction of crack propagation is consistent with the river-like flow pattern.

Table 1
Mechanical properties of the Ti–Zr–Ni–Cu–Y alloys and other containing i-phase alloys.

Alloys	Phase constituent	Hv and corresponding load (N)	Compressive strength σ_f (MPa)	Deformation at fracture ε (%)	Young's modulus E (GPa)
$Ti_{48}Zr_{36}Ni_{14}Cu_2$	i + L	$509 \pm 8/4.9$	1138	5.02	22.6
$(Ti_{48}Zr_{36}Ni_{14}Cu_2)_{0.99}Y_{0.01}$	i + L	$528 \pm 5/4.9$	1351	6.12	21.7
$(Ti_{48}Zr_{36}Ni_{14}Cu_2)_{0.98}Y_{0.02}$	i + L + β	$537 \pm 19/4.9$	1248	5.62	22.2
$Ti_{60}Zr_{20}Ni_{20}$ [23]	i + L + α	546/1.96	750	2.1	35.7
$Ti_{60}Zr_{25}Ni_{15}$ [23]	i + α	504/1.96	960	4.2	22.9
$Ti_{40}Zr_{40}Ni_{20}$ [24]	i	520/1.96	542	1.25	43
$Ti_{41.5}Zr_{41.5}Ni_{17}$ [22]	i	630/4.9	–	–	–
$Ti_{45}Zr_{35}Ni_{17}Cu_3$ [4]	i	620/4.9	1030	8	12

i, icosahedral quasicrystalline phase; L, C14 Laves phase; $\beta(\alpha)$, solid solution phase.
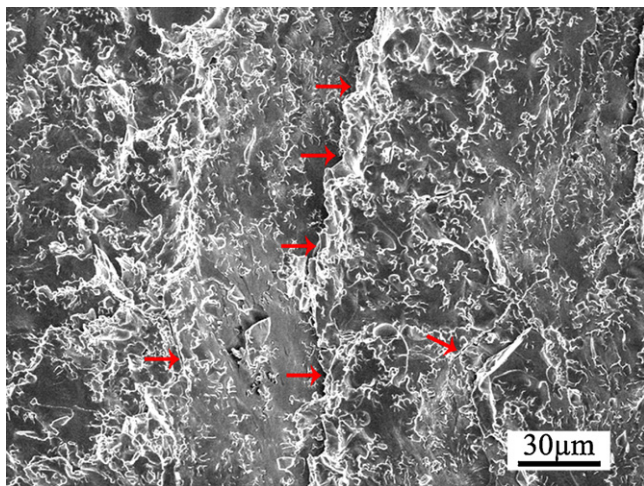
Fig. 6. The fracture surface appearance of the bulk $(Ti_{48}Zr_{36}Ni_{14}Cu_2)_{0.99}Y_{0.01}$ alloy.
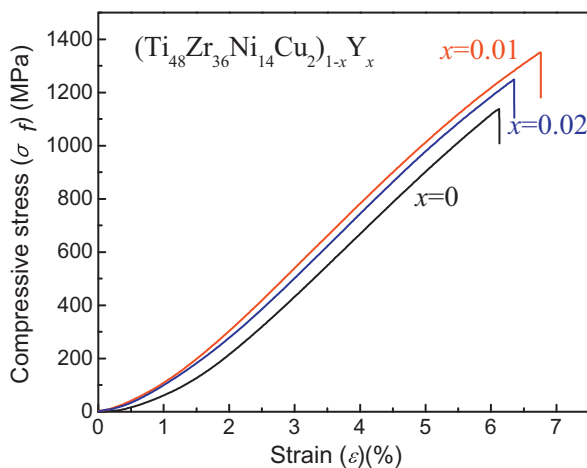
Fig. 5. The compressive curves of the bulk $(Ti_{48}Zr_{36}Ni_{14}Cu_2)_{1-x}Y_x$ ($x = 0$, 0.01 and 0.02) alloys.

4. Conclusions

The structure of as-cast $(Ti_{48}Zr_{36}Ni_{14}Cu_2)_{1-x}Y_x$ ($x = 0$, 0.01 and 0.02) alloys is mainly composed of the i-phase, coexisting with L-phase or β-(Ti, Zr) phase. All the alloys have the elastic deformation at room temperature, and the fracture mode is brittle cleavage fracture. Appropriate amount of Y addition leads to an increase in fracture strength and microhardness. The maximum compressive fracture strength of 1351 MPa and good elastic deformation

of 6.12% is exhibited in the $(Ti_{48}Zr_{36}Ni_{14}Cu_2)_{0.99}Y_{0.01}$ alloy. With regards to the microhardness test, no obvious crack is detected even at the load of 4.9 N, which suggests that these alloys have better toughness. The Y element addition in the as-cast Ti-based i-phase alloys showing good forming ability and higher mechanical properties, which might provide clues for designing high strength new type Ti-based alloys.

References

[1] D. Shechtman, I. Blech, D. Gratias, J.W. Cahn, Phys. Rev. Lett. 53 (1984) 1951–1953.
[2] K.F. Kelton, P.C. Gibbons, P.N. Sabes, Phys. Rev. B 38 (1988) 7810–7813.
[3] K.F. Kelton, W.J. Kim, R.M. Stround, Appl. Phys. Lett. 70 (1997) 3230–3232.
[4] B. Liu, Y. Wu, L. Wang, J. Non-Cryst. Solids 352 (2006) 3936–3941.
[5] L. Wang, C. Li, L. Ma, A. Inoue, J. Alloys Compd. 339 (2002) 216–220.
[6] B. Liu, G. Fan, Y. Wang, Y. Wu, L. Wang, Int. J. Hydrogen Energy 33 (2008) 5801–5805.
[7] B. Liu, J. Liu, G. Mi, Z. Zhang, Y. Wu, L. Wang, J. Alloys Compd. 475 (2009) 881–884.
[8] A. Matsumoto, K. Kobayashi, T. Nishio, K. Ozaki, J. Metastable Nanocrystal. Mater. 24–25 (2005) 335–338.
[9] A. Matsumoto, K. Kobayashi, T. Nishio, K. Ozaki, J. Alloys Compd. 434–435 (2007) 315–318.
[10] P.A. Bancel, P.A. Heiney, A.I. Goldman, P.M. Horn, Phys. Rev. Lett. 54 (1985) 2422–2425.
[11] R.M. Stroud, K.F. Kelton, J. Mater. Res. 12 (1997) 434–438.
[12] L.Z. Zhu, D. Shan, Y. Jin, X. Huang, Trans. Mater. Heat Treat. 27 (2006) 108–113.
[13] X. Zhang, R.M. Stroud, J.L. Libbert, K.F. Kelton, Philos. Mag. B 70 (1994) 927–950.
[14] K.N. Ishihara, Mater. Sci. Forum 22–24 (1987) 223–230.
[15] A.I. Goldman, K.F. Kelton, Rev. Mod. Phys. 65 (1993) 213–230.
[16] K. Chattopadhyay, S. Lele, R. Prasad, S. Ranganathan, G.N. Subbanna, N. Thangaraj, Scripta Metall. 19 (1985) 1331–1334.
[17] P.C. Gibbons, K.F. Kelton, L.E. Levine, R.B. Phillips, Philos. Mag. B 59 (1989) 593–598.
[18] W.J. Kim, K.F. Kelton, Philos. Mag. A 72 (1995) 1397–1408.
[19] P.M. Sargent, in: P.J. Blau, B.R. Lawn (Eds.), Microindentation Techniques in Materials Sciences and Engineering, ASTM STP 889, Philadelphia, USA, 1986, p. 160.
[20] G.V.S. Murthy, A.K. Ray, R.K. Minz, N.K. Mukhopadhyay, J. Mater. Sci. Lett. 18 (1999) 255–258.
[21] N.K. Mukhopadhyay, G.C. Weatherly, J.D. Embury, Mater. Sci. Eng. A 315 (2001) 202–210.
[22] S. Yi, K.B. Kim, E. Fleury, W.T. Kim, D.H. Kim, Mater. Lett. 52 (2002) 75–79.
[23] J.B. Qiang, Y.M. Wang, L.J. Yuan, D.J. Li, C. Dong, Acta Metall. Sinica 40 (2004) 62–66.
[24] J.B. Qiang, Z. Wei, H.G. Huang, N. Jiang, C. Dong, Acta Phys. Sinica 54 (2005) 1909–1913.
[25] C. Dong, Quasicrystalline Materials, National Defence Industry Press, Beijing, 1998, p. 159.
[26] Y. Yokoyama, A. Inoue, T. Masumoto, Mater. Trans. JIM 34 (1993) 135–145.
[27] U. Ponkratz, R. Nicula, A. Jianu, E. Burkel, J. Phys.: Condens. Matter 12 (2000) 8071–8080.